ICRC'07
Mérida, México

Status of the RICE Experiment

ILYA KRAVCHENKO[1], J. ADAMS[2], A. BEAN[3], D. BESSON[3], S. CHURCHWELL[2], P. HARRIS[2], S. HUSSAIN[4], D. HOGAN[3], D. MARFATIA[3], D. MCKAY[3], J. RALSTON[3], S. RAZZAQUE[5] (*presenter*), D. SECKEL[4], S. SEUNARINE[4], R. SCHIEL[3].

[1]*Massachusetts Institute of Technology for Nuclear Science, Cambridge, MA 02139*

[2]*Department of Physics and Astronomy, Private Bag 4800, U. of Canterbury, Christchurch, New Zealand*

[3]*Dept. of Physics and Astronomy, University of Kansas, Lawrence, KS*

[4]*Department of Physics and Astronomy and Bartol Research Institute, U. of Delaware, Newark DE 19716*

[5]*Department of Astronomy and Astrophysics and Department of Physics, Pennsylvania State University, University Park, PA 16802*

dbesson@ku.edu

Abstract: We report on recent results from the RICE experiment, located at the South Pole. This includes an updated limit on the neutrino flux in the range 10-1000 PeV, first results on a search for gamma-ray burst coincidences, and a search for highly relativistic, ionizing magnetic monopoles.

Introduction

The RICE experiment has goals similar to the larger ICECUBE[1] experiment - both seek to measure UHE neutrinos by detection of Cherenkov radiation produced by $\nu_l + N \rightarrow l + N'$. Whereas ICECUBE is optimized for detection of penetrating muons resulting from $\nu_\mu + N \rightarrow \mu + N'$, RICE is designed to detect compact electromagnetic cascades initiated by $e^+(/e^-)$: $\nu_e(/\overline{\nu}_e) + N \rightarrow e^\pm + N'$. As the cascade develops, atomic electrons in the target medium are swept into the forward-moving shower, resulting in a net charge on the shower front of $Q_{tot} \sim E_s e/4$; E_s is the shower energy in GeV. Such cascades produce broadband Cherenkov radiation – for $\lambda^{Cherenkov}_{E-field} \gg r_{Moliere}$, the emitting region approximates a point charge of magnitude Q_{tot} and therefore emits fully coherently. Experimental sensitivity is enhanced by the radio transparency of cold ice – the field attenuation length at such wavelengths $\sim$1 km. One calculation finds[2] that, for $E_{\nu_e} >$1 PeV, radio detection of neutrino-induced cascades becomes more cost-effective than PMT-based techniques.

Methods

The RICE experiment presently consists of a 20-channel (16-channel for the data discussed herein) array of dipole radio receivers ("Rx"), scattered within a 200 m×200 m×200 m cube, at 100-300 m depths. The signal from each antenna is boosted by a 36-dB in-ice amplifier, then carried by coaxial cable to the surface observatory, where the signal is filtered (suppressing noise below 200 MHz), re-amplified (either 52- or 60-dB gain), and split - one copy is fed into a CAMAC crate to form the event trigger; the other signal copy is routed into one channel of an HP54542 digital oscilloscope. Short-duration pulses broadcast from under-ice transmitters provide the primary calibration signals, and are used to verify vertex reconstruction techniques. Two vertex-reconstruction algorithms identify putative sources. One algorithm searches a grid around the array for the source point most consistent with the observed hit times; the second technique analytically solves for the vertex using four-hit subcombinations of all the available hits[3].

The primary physics goal of RICE is detection of UHE cosmic ray neutrinos. In the energy range $E_\nu \sim 10^{15-17}$ eV, AGN sources are believed to
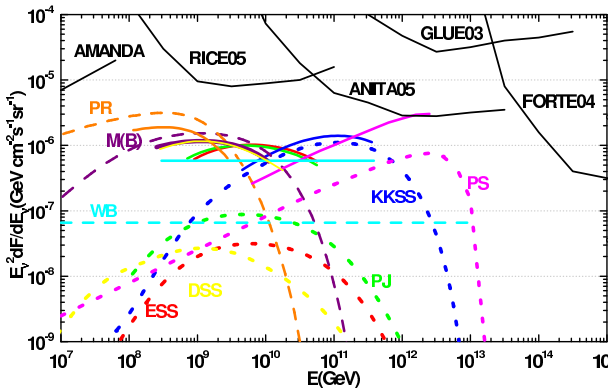
Figure 1: Upper bounds on total (all flavor) neutrino fluxes for cosmogenic neutrino models of DSS[11], ESS [6], PJ [5], and KKSS [7], and AGN core models of Protheroe PJ [8] and Mannheim PJ [9]due to all flavor NC+CC interactions, based on 1999-2005 RICE live-time of about 13200 hrs. Dot and dash curves are the model fluxes; thick solid curves are the corresponding bounds (95% for RICE; 90% for other experiments).

dominate; at higher energies, the "GZK"[4] flux is calculable, given some assumptions regarding the redshift distribution, source evolution, and energy spectrum at the source. Since RICE data-taking began over seven years ago, no convincing neutrino candidates have survived, allowing bounds to be placed on the incident neutrino flux at Earth. Figure 1 shows the comparison of our results with three cosmogenic [4] neutrino models [5, 6, 7], two AGN jet models [8, 9][1], and the corresponding upper bounds on the fluxes based on the RICE 1999-2005 live-time and effective volume estimates. An additional 25% of livetime accumulated since that time in 2006-07 has not yet been completely analyzed and therefore not yet incorporated into these results. The all-flavor bounds (based on Standard-Model event rates) are computed for the energy region corresponding to the inner 80% of the shower rate; the models of [6] and [7] serve as two extreme cases. We note that the current RICE bound is of the same order as many predictions.

Coincidences with GRBs We have investigated the possibility of coincidences of RICE events with Gamma Ray Bursts[12]. Given the uncertainty in
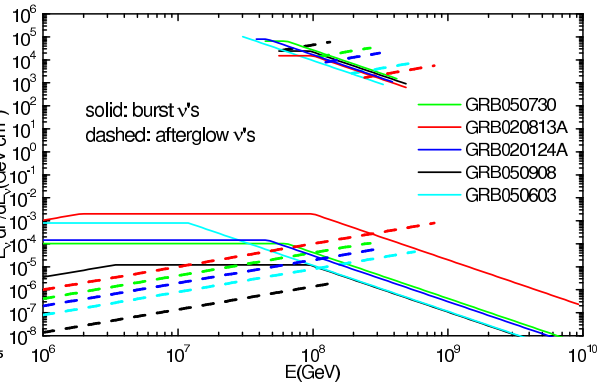

Figure 2: RICE upper bounds on neutrino fluxes from point source gamma-ray bursts. Upper bounds on the diffuse GRB flux are published elsewhere[13].

the time delay between the optical and the neutrino signals expected from GRBs, we have considered a GRB coincidence candidate to be any RICE event within ±1000 sec of the time recorded for a GRB. Due to the opacity of the earth to UHE neutrinos, RICE is only sensitive to GRBs localized in the southern hemisphere. Over 2000-2005, there were approximately 100 such GRBs which satisfied this criterion. Only five events have sufficient spectral information to allow an extraction of the neutrino flux from the recorded GRB luminosity and redshift data (Figure 2). Unfortunately, since this small sample is a predominantly high-redshift sample, limits are still considerably weaker than the expected flux. Future coincident measurements are important as GRB observations improve in both frequency and quality.

Relativistic Intermediate Mass Monopoles (IMM)

IMM's are expected to reach highly relativistic velocities. Wick et al.[14] presented a toy model of magnetic monopoles traversing intergalactic magnetic fields. By treating magnetic monopole motion as a three-dimensional random walk induced by randomly-aligned patches of roughly coherent magnetic fields, they estimated that IMM's cre-

---

1. These AGN jet models are ruled out by the WB bound [10] for optically thin sources but are still allowed by direct neutrino experiments.

ated in the early universe would now have typical kinetic energies on the order of 10^{16}GeV and $\gamma = 10^{11}$. The fact that IMM's reach such "ultrarelativistic" γ values provides a mechanism for their detection, given the electromagnetic shower "wake" that follows the monopole. It is through detection of such ionization that RICE searches for intermediate-mass monopoles.

Energy loss The model of monopole energy loss used is based on the muon/tau energy loss model of Dutta et al.[15]. Dominant energy loss mechanisms are photonuclear interactions, pair production and bremstrahlung. Although energy loss due to ionization can be treated as smooth and continuous with little loss of accuracy, we explicitly model the stochastic fluctuation in pair production and photonuclear energy losses. We approximate the energy loss for a given process i (brem., pair, or photonuclear) over a small distance Δx as:

$$\Delta E_i \approx \sum_{j_{y_j=y_{min}}}^{y_j=y_{max}} \frac{N}{A}(y_j E)\left(\Delta x \frac{d\sigma_i}{dy_j}\right)\Delta y \quad (1)$$

Recasting the energy loss equation this way effectively sorts the total energy loss into an arbitrary number of bins, each of which spans a length Δy of the possible inelasticity (y) values. Since y_j is the fractional energy loss in a single interaction within bin j and E is the total energy of the particle, $(y_j E)$ is the energy loss for a single interaction in the jth bin. Each term of the Riemann sum represents an energy loss, so if $(y_j E)$ is the energy loss in a single interaction, the expectation number of interactions in the jth bin is given by:

$$\langle n_{ij} \rangle = \frac{N}{A}\Delta x \frac{d\sigma_i}{dy_j}\Delta y \quad (2)$$

Generalization to monopoles

We now convert this stochastic model of muon energy loss to a model of magnetic monopole energy loss in matter. First, the muon mass must be replaced by the magnetic monopole mass wherever muon mass appears in the equations for α and the β_i's. Because bremsstrahlung falls off inversely with particle mass, the bremsstrahlung energy loss contribution is negligible for even

light magnetic monopoles and will be subsequently disregarded[14]. It should be noted that at large masses ($>$1TeV), $\beta_{\text{pair production}}$ can become difficult to calculate numerically due to rounding error; however, pair production energy loss approaches an asymptotic limit with increasing particle mass and varies with mass by only a few percent for masses above $\approx$ 100 MeV.

Flux upper bounds

The standard RICE Monte Carlo simulation used to assess the sensitivity to neutrino-induced cascades has been modified to determine the effective area for detection of monopoles. Ionizing monopoles are simulated over 4π sr since the Earth is not entirely opaque to monopoles below the horizon. The RICE signal detection efficiency is also degraded by 15% to account for ice birefringence effects, which reduce the average peak signal voltage recorded by the data acquisition system. Upper limits are presented in Figure 4.

Future Plans

Owing to its high purity, South Polar ice is among the most transparent on the planet. The unparalleled infrastructure make future expansion of the radio technique the South Pole particularly attractive. Running through 2009 should improve the RICE sensitivity by a factor of two. Beyond that, simulations indicate that 2–5 "GZK" neutrinos (assuming the ESS flux) are achievable at a hardware cost of ~5M. The AURA initiative, described elsewhere in these proceedings, seeks development of that next-generation radiofrequency neutrino detector. Other strategies are also being developed.

References

[1] arXiv:0705.1781, and references cited therein.
[2] P. B. Price (UC, Berkeley), astro-ph/9510119, published in Astropart. Phys. 5, 43, (1996).
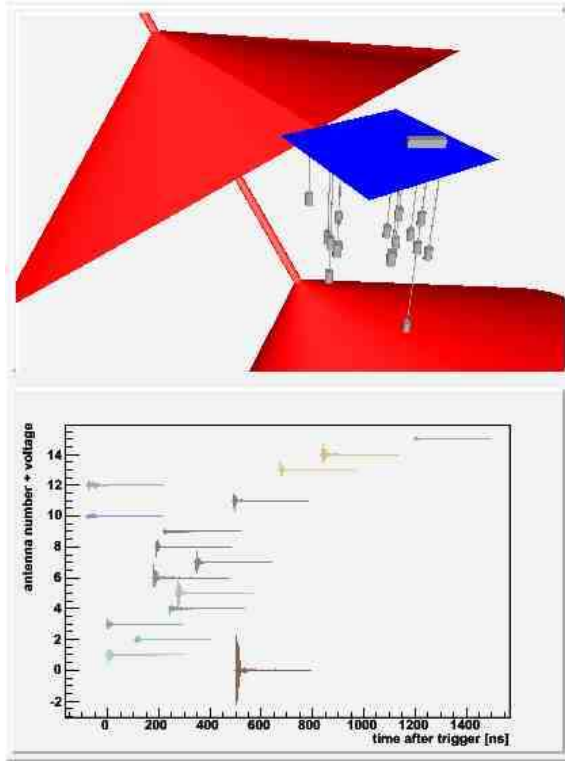[3] arXiv:0705.4491, I. Kravchenko et. al. (2007).

Figure 4: Preliminary monopole flux bounds.

[4] K. Greisen, Phys. Rev. Lett. **16**, 748 (1966); G. Zatsepin and V. Kuzmin, Pis'ma Zh. Eksp. Teor. Fiz. **4**, 114 (1966); JETP Lett. **4**, 78 (1966).

[5] R. Protheroe and P. Johnson, Astropart. Phys. **4**, 253 (1996).

[6] R. Engel, D. Seckel, and I. Stanev, Phys. Rev. **D64**, 093010 (2001).

[7] O. E. Kalashev, V. A. Kuzmin, D. V. Semikoz, and G. Sigl, Phys. Rev. **D66**, 063004 (2002).

[8] R. J. Protheroe, arXiv:astro-ph/9607165.

[9] K. Mannheim, Astropart. Phys. **3**, 295 (1995); V. Berezinsky and G. Zatsepin, Phys. Lett. **28B**, 423 (1969); F. W. Stecker, Astrophys. J. **228**, 919 (1979).

[10] J. Bahcall and E. Waxman, Phys. Rev. **D59**, 023002 (1998); Phys. Rev. D **64**, 023002 (2001).

[11] Daniel De Marco, Todor Stanev, and F.W. Stecker, arXiv:astro-ph/0512479.

[12] D. Besson et. al., Astropart.Phys. 26 (2007) 367-377

[13] I. Kravchenko et al., Phys. Rev. **D73** (2006) 082002

[14] S.D. Wick, T.W. Kephart, T.J. Weiler, and P.L. Biermann, Astropart. Phys. **18**, 663 (2003).

[15] S.I. Dutta, M.H. Reno, I. Sarcevic, and D. Seckel, Phys. Rev. **D63**, 094020 (2001)

Figure 3: Two views of a typical downgoing monopole (mass= 10^7 PeV, $\gamma = 10^8$) interacting on the surface and passing near RICE: (a) Physical view. (b) Voltage vs. time (as measured at the DAQ) in each RICE antenna channel as caused by the same monopole. The voltage graphs for the different antennas have been shifted vertically for clarity; the flat-line portion of each individual graph corresponds to 0V. The frequency-dependent RICE transfer function has been convolved with the shower spectral characteristics at the antenna to yiel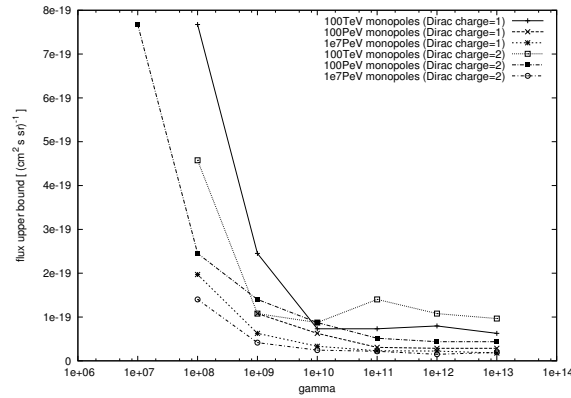d (after Fourier transform) the time-domain waveform shown.